島根大学地球資源環境学研究報告　19, 101～112 ページ（2000 年 12 月）
Geoscience Rept. Shimane Univ., 19, p.101～112（2000）

Whole-rock elemental abundances in sandstones and mudrocks from the Tanabe Group, Kii Peninsula, Japan

Barry Roser*, Jun-Ichi Kimura* and Kunihiko Hisatomi**

Abstract

Siliciclastic sediments of the Lower Miocene Tanabe Group crop out in southwest Kii Peninsula, Wakayama Prefecture, and represent a forearc basin succession deposited on the uplifted Shimanto accretionary complex. This report contains whole-rock XRF data for a stratigraphic collection of 87 sandstones and mudrocks from the Tanabe sequence. Fifty-four samples have also been analysed for REE and additional trace element by solution ICP-MS after acid digestion and alkali fusion. The results show characteristic elemental sorting fractionation between sandstones and mudrocks in the members of the basal Asso Formation, which becomes more marked in the overlying Shirahama Formation, probably as a result of winnowing in a storm-dominated shelf depositional environment. Elemental abundances generally compare well with those of the Shimanto protoliths from which the Tanabe Group was derived.

Introduction

The Lower Miocene Tanabe Group outcrops extensively in southwest Kii Peninsula, Wakayama Prefecture (Fig. 1). The Tanabe succession has a maximum thickness of about 1500 m, and comprises a varied assemblage of siliciclastic sediments including mudstone, sandstone – mudstone alternations, massive sandstone, conglomerate and breccia (Tanabe Research Group 1984). The Tanabe Group rests unconformably on the Otonashigawa and Muro Groups of the Shimanto terrane, and was deposited in a shallow-water forearc basin, similar to modern equivalents at the SW Japan Pacific margin.

The Tanabe sequence represents the Miocene stage of evolution of the inboard and underlying Shimanto accretionary wedge. This report contains whole rock XRF and ICP-MS analyses of a stratigraphic collection from the Tanabe Group, to complement earlier sampling from the Shimanto terrane proper (Roser et al. 1998a). The purpose of both collections is to examine the Cretaceous to Miocene evolution of the SW Japan subduction margin. The main aim of this report is to present the data, briefly outline the analytical techniques used, and describe broad elemental abundances and variations within the Tanabe Group. Analysis of a number of elements by both XRF and ICP-MS also allows comparison between the techniques. More detailed discussion of provenance signatures, effects of recycling, and the influence of depositional environment on the geochemistry of the sequence will be published elsewhere (Roser et al. in prep). Preliminary interpretation has been presented by Roser et al. (2000).

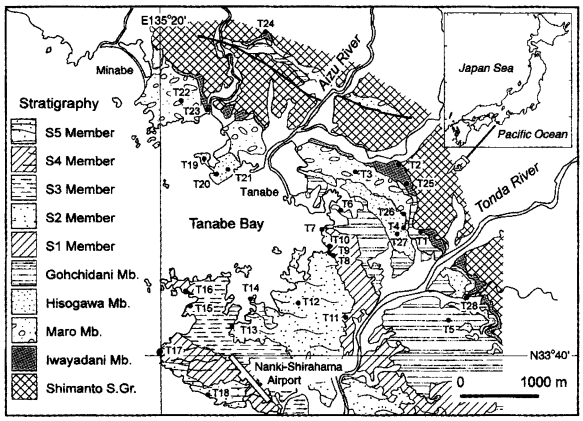

Fig. 1. Location map showing distribution of the Tanabe Group in Kii Peninsula and sample sites.

Geological Outline and Sample Suites

1. Tanabe Group

The Tanabe Group has been studied in detail by the Tanabe Research Group (TRG). They mapped the area, refined the stratigraphy, carried out detailed facies analysis, and constructed an integrated basin model, particularly of the lower half of the sequence (TRG 1984, 1985, 1992, 1993). The geological summary below is largely drawn from that work, supplemented by field observation during sample collection.

The Tanabe Group is subdivided into the Asso and Shirahama Formations. The basal Asso Formation is further divided into the Iwayadani, Maro, Hisogawa, and Gohchidani Members, in ascending order (Fig. 2). The Iwayadani Member rests unconformably on Shimanto terrane sediments, and consists of subangular to angular

* Dept of Geoscience, Faculty of Science & Engineering, Shimane University, Matsue 690-8504
**Dept of Earth Sciences, Faculty of Education, Wakayama University, Wakayama 640-8510

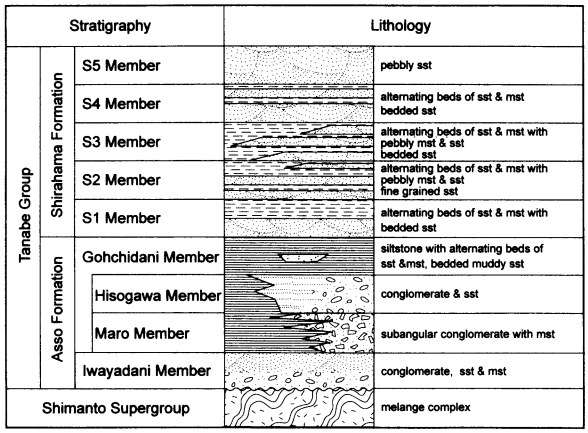

Fig. 2. Schematic stratigraphy of the Tanabe Group, after Tanabe Research Group (1992, 1993).

conglomerates with sandy matrix, sandstones, and mudstones, and occasional coaly horizons. The Iwayadani Member thins from north to south, and has been interpreted as drowned valley fill. It is succeeded by conglomerates and mudstones of the Maro and Hisogawa Members, which occur only in the north of the Tanabe outcrop area. The Maro Member consists of subangular conglomerates with sandy matrix, along with mudstones. The Hisogawa Member comprises sandy conglomerates, sandstones and siltstones. All three lower members interfinger with mudstones and siltstones of the lower Gohchidani Member to the south. The Hisogawa Member is overlain by upper Gohchidani mudrocks with occasional sandy alternations. Clasts in the Asso conglomerates are dominated by Shimanto sandstones, thought to be of Otonashigawa Group derivation in the Iwayadani Member, and from the Muro Group in the Maro and Hisogawa Members.

Facies arrangements in the Asso Formation are interpreted as a fan delta complex, with the conglomeratic members representing proximal deposition from a northerly source, passing to more distal muds and silts in the lower Gohchidani Member to the south. Distinct stages of genesis, progradation, aggradation and abandonment of the fan delta complex are recognised from facies analysis (TRG 1993). These stages are roughly equivalent to the contrasting facies in the Iwayadani, Maro, Hisogawa, and upper Gohchidani, respectively. The Asso sequence overall is related to a transgressive phase which in turn consists of three short-term phases: that is, transgressive phase (Hisogawa member), highstand phase (Maro and Hisogawa Members) and then transgressive phase (upper Gohchidani Member).

The Shirahama Formation is divided into five broadly defined fining-upwards members, designated S 1 through S 5 (Fig. 2). In contrast to the Asso Formation, the Shirahama Formation consists primarily of bedded sandstone, sandstone-mudstone alternations, and rarer conglomerates, sandstones and pebbly mudstones. The S 1 Member marks the first appearance of quartzose schist clasts, in contrast to the Shimanto clasts that dominate in the Asso Formation. Quartz rock fragments and acid volcanics are also significant components in the clast populations, and sandstones are subordinate.

Sandstone packets thin to the south and proportions of mud increase (Fig. 2), reflecting a facies arrangement with respect to a NE to WNW source similar to that of the Asso Formation. Although many sandstones show parallel lamination, hummocky cross-bedding and planar cross-bedding, other sedimentary structures are common, including swaley cross-bedding; storm deposits are also recognised (TRG 1985; Shimizu & Hisatomi 1993). These features suggest shallow water deposition, including intertidal environments. Mudstone dikes and sills also occur in some areas (Shimizu 1985).

The Tanabe Research Group (1985) described the Shirahama Formation as shallow marine sediments accumulated on the continental shelf during a regressive phase. The Tanabe Group sequence overall is also not dissimilar to the generally shoaling-upward sequence seen in the filling of ridge-confined forearc basins. Lateral facies variations are also similar to such sequences. The stratigraphy of the Shirahama Formation is currently being revised using detailed sedimentary facies analysis (Hisatomi 1998), similar to that carried out earlier for the Asso Formation. This work has recognised a number of upward coarsening megacycles, in contrast to the lithostratigraphic divisions made previously. Because this revision is still in progress, we have here used the older TRG divisions.

2. Sample Suites

A total of 87 Tanabe Group sandstones and mudrocks were collected during fieldwork in October-November 1999. The sampling strategy was intended to collect roughly equal numbers of sandstones and mudrocks from each member of both the Asso and Shirahama Formations, to cover the observed range in lithotype. In practice, this proved to be difficult, with finer size grades underrepresented in the conglomeratic horizons in the Asso Formation. To partially overcome this, laterally equivalent mudstones were collected from the more distal lower Gohchidani Member. The majority of the Asso Formation samples were collected from inland exposures in the north of the Tanabe outcrop area, whereas most Shirahama samples were collected from coastal outcrop in the southwest (Fig. 1).

Sample preparation

Lithified samples were chipped to <10 mm maximum diameter using a manual rock splitter. Many of the mudstones and siltstones were friable or blocky, and no

splitting was required. Chip containing veins or surficial oxidation was discarded after washing in running city water to remove loose surface material. The samples were then soaked in deionised distilled water for 24-36 hours, with several changes of water in that time. The cleaned samples were then dried overnight in an oven at 110°C before crushing. The samples were crushed in a tungsten carbide ring mill, in loads of 70-150 g. Maximum mill times were <60 seconds for the sandstones, and as little as 15 seconds for some unlithified siltstones and mudstones. Such mill times are sufficient to produce powders as fine or finer than by agate mortar systems, with no contamination except for tungsten and cobalt (Roser et al. 1998b). Subsamples of the resulting pulps were then dried in an oven at 110°C for at least 24 hours prior to determination of loss on ignition (LOI).

LOI determinations were made by weighing 5-6 g of dried sample into ceramic crucibles, followed by ignition in an electric furnace at 1000°C for two hours. LOI was then calculated from the net weight loss. The ignited material was then manually disaggregated and recrushed in an agate pestle and mortar, and returned to a 110°C oven for at least 24 hours. This ignited material was used for preparation of both the fusion beads for X-ray fluorescence analysis and the solutions for ICP-MS analysis.

Analytical Methods

Analyses of major elements and 14 trace element were made using a Rigaku RIX-2000 XRF at Shimane University. All analyses were carried out on glass beads prepared in an automatic bead sampler, using an alkali flux comprising 80% lithium tetraborate and 20% lithium metaborate, with a sample to flux ratio of 1:2. Analytical methods, instrumental conditions and calibration follow those described by Kimura and Yamada (1996). Analyses were monitored by repeat analyses of several GSJ standards, from new beads not included in the calibration. Trace element results were also tested by cross-calibration against new analyses of a suite of 14 Shimanto sandstones and mudrocks from Roser et al. (1998a).

Based on the XRF results, 54 samples were selected for analysis of REE and additional trace elements by solution ICP-MS. Samples were analysed in batches of 20 per day, including one blank and one to three GSJ rock standards. Solutions were prepared using a combined alkali fusion and acid digestion procedure (AFAD), which will be described in detail by Kimura et al. (in prep.). Briefly, the method consists of digestion of 0.1000 g oven-dried sample with 1.0 ml $HClO_4$ and 1.0 ml 40% HF, in Pt crucibles heated to 200°C on a hot plate. This digest is evaporated to dryness over 3 hr, and 0.5 g anhydrous Na_2CO_3 alkali flux is then added. The crucibles are then heated for 10 minutes in an electric furnace at >900°C. The fluxed samples are then partially dissolved in the Pt crucibles by addition of 5 ml HNO_3 and several drops of HF, heated on a hot plate for 10 minutes at 100°C, followed by addition of 10 mls deionized distilled water and 20 minutes further heating. The resulting solutions are then quantitatively transferred to weighed 100 ml polyethylene bottles, with the residue (if any) retained in the crucibles. A third digestion is then carried out by addition of 10 mls HCl, several drops of HF, and 5 mls deionized water, followed by heating at 150°C for at least 30 minutes to dissolve any remaining residue. This last step is important for high field strength element (HFSE) recovery. In the case of the Tanabe samples little residue was present at the beginning of this step, and any present dissolved well before the 30 minutes heating had elapsed. The resulting solution is then quantitatively added to the polyethylene bottles, and the solution made up to 100 ml (by weight) by addition of deionized water. These stock solutions are stable for several weeks at room temperature, and are subsequently diluted 50,000x for conventional solution ICP-MS analysis.

One 100 ml bottle of procedural blank solution was prepared for each daily batch of solution analyses, along with two 10 ml tubes of solution for each unknown sample or standard rock. One ppb equivalent In (indium) was added to the blank solution and all sample tubes for internal standardization. One ppb equivalent (50 ppm equivalent in original samples) of multi-element mixed standard solution (SPEX Co.) was added to one of the 10 ml tubes of each unknown sample. Elemental concentrations in the unknowns were determined by standard addition method using the blank, sample, and standard addition samples described above. The ICP-MS used was the VG PQ3 at Shimane University, operated in normal nebulization mode. Measurement conditions are: RF power of 1350 W (reflection power = 0), nebulizer gas flow rate 0.7 l/min, intermediate gas flow rate 1.3 l/min, and cooling gas flow rate 13 l/min. Peak jumping mode was used, with three points measured for each mass peak at a dwell time of 10 msec. Three 60 sec acquisitions are applied to the blank, sample and standard addition sample. Isobaric oxide molecular interferences were corrected using correction factors determined from mixed standard solutions. Detail of the analytical procedure will be given in a separate paper (Kimura et al., in prep.).

Results and Discussion

XRF major and trace element results are given in Table 1, listed on a hydrous basis. The ICP/MS results are given in Table 2. Lithology for each sample was estimated from hand specimens using a hand lens and grain size comparator.

Table 1 XRF major and trace element analyses of Tanabe Group sandstones, siltstones and mudstones, Kii Peninsula. Major elements wt%, trace elements p.p.m. LOI=loss on ignition. LITH=lithology (CS=coarse grained sst; MS=medium sst; FS=fine sst; VFS=very fine sst; CZ=coarse siltstone; ZST=siltstone; MST=mudstone).

SA#	LITH	SiO_2	TiO_2	Al_2O_3	Fe_2O_3T	MnO	MgO	CaO	Na_2O	K_2O	P_2O_5	LOI	Total	Ba	Ce	Cr	Ga	Nb	Ni	Pb	Rb	Sc	Sr	Th	V	Y	Zr
Asso Formation																											
Iwayadani Member																											
IW1	MS	85.15	0.11	7.25	1.88	0.04	0.45	0.39	1.41	1.18	0.02	2.15	100.02	233	19	11	6	1	7	13	41	2.2	70	4.9	17	10	78
IW2	MS	82.23	0.09	10.14	0.43	0.00	0.17	0.05	1.90	3.45	0.01	0.90	99.37	581	34	12	9	1	<1	20	91	1.4	89	5.4	12	12	74
IW3	MS	83.58	0.07	9.59	0.64	0.01	0.15	0.04	1.63	3.24	0.01	0.99	99.94	516	18	8	9	1	1	17	89	1.4	72	4.2	9	7	77
IW4	CS	79.86	0.21	9.61	1.71	0.03	0.43	1.27	1.63	2.05	0.05	2.71	99.55	343	28	18	8	3	10	15	69	3.5	113	6.1	32	11	99
IW5	FS	76.90	0.30	11.41	2.51	0.03	0.60	0.73	1.44	2.52	0.05	3.26	99.75	309	30	31	11	5	12	16	86	5.5	115	7.3	51	15	114
IW6	CS	77.36	0.26	10.63	1.81	0.03	0.82	1.60	1.65	2.27	0.04	3.68	100.14	337	24	18	10	5	9	15	76	5.7	107	5.6	43	11	101
IW7	CZ	71.51	0.44	13.88	3.36	0.03	0.79	0.71	1.46	3.18	0.05	4.30	99.71	357	41	38	14	8	17	19	111	6.6	122	9.2	67	16	125
Maro Member																											
MA1	MST	66.18	0.46	13.78	6.23	0.11	1.48	0.46	1.80	2.93	0.07	6.03	99.52	508	51	37	12	8	15	15	110	8.8	120	13.6	79	30	186
MA2	FS	75.24	0.30	11.22	2.63	0.03	1.00	1.07	1.69	2.20	0.03	4.31	99.72	348	36	25	10	4	13	14	84	6.5	108	10.0	50	18	107
MA3	MST	66.94	0.54	14.76	5.03	0.11	1.36	0.45	1.72	3.13	0.05	5.78	99.85	410	48	49	14	10	21	22	122	10.5	102	13.2	97	27	161
MA4	MST	64.80	0.60	14.73	5.15	0.04	1.61	1.55	1.64	3.24	0.09	6.48	99.91	556	48	56	15	11	22	21	133	11.2	172	13.3	98	27	150
MA5	CZ	68.82	0.53	14.16	4.77	0.09	1.36	0.52	1.83	2.93	0.05	5.36	100.40	337	50	46	16	10	17	15	109	9.4	124	8.9	91	23	177
MA6	VFS	72.13	0.42	11.96	3.90	0.12	1.32	0.84	1.76	2.38	0.06	4.78	99.66	312	33	33	12	5	19	13	86	8.8	119	8.5	79	17	123
MA7	VFS-CZ	71.95	0.43	12.53	4.16	0.12	1.27	0.74	1.71	2.46	0.05	4.62	100.03	318	34	41	13	5	18	10	89	9.0	117	9.3	86	18	128
MA8	CZ	68.29	0.57	15.18	4.26	0.09	1.23	0.36	1.69	3.17	0.06	4.89	99.80	355	48	51	15	10	24	15	111	9.8	119	11.7	95	21	180
MA9	FS	71.95	0.41	11.94	4.09	0.12	1.33	0.94	1.74	2.35	0.05	4.92	99.84	316	34	40	12	7	20	12	86	9.2	121	9.5	75	17	102
MA10	CZ	73.21	0.61	15.63	1.22	0.01	0.70	0.07	1.92	3.14	0.03	3.17	99.71	289	52	45	16	10	9	11	117	8.9	80	10.9	89	22	153
MA11	CZ	77.49	0.43	13.24	0.85	0.01	0.45	0.11	1.80	2.96	0.02	2.45	99.81	491	49	29	13	8	9	17	109	5.5	108	9.8	59	18	169
MA12	VFS	78.07	0.36	12.47	0.90	0.01	0.42	0.11	1.94	2.81	0.02	2.35	99.45	443	44	26	13	6	5	21	104	4.9	109	8.4	50	16	138
Hisogawa Member																											
HS1	FS	80.39	0.23	10.24	2.14	0.03	0.58	0.51	1.41	2.15	0.04	2.75	100.48	341	33	20	11	6	9	12	74	3.9	98	5.5	34	15	98
HS2	FS	71.18	0.25	9.88	3.74	0.08	1.41	3.38	0.99	2.14	0.05	6.70	99.80	335	35	19	9	6	11	13	75	10.4	96	8.9	49	20	108
HS3	CZ	63.71	0.44	13.17	12.13	0.15	1.05	0.21	0.83	3.24	0.06	4.99	99.99	368	46	38	16	10	14	20	110	18.0	68	9.5	124	32	185
HS4	CZ	69.06	0.51	14.34	5.86	0.07	0.82	0.21	1.56	3.36	0.06	3.93	99.77	380	56	41	15	10	13	18	123	10.6	85	12.3	99	28	182
HS5	FS	75.26	0.29	11.37	3.51	0.06	0.89	1.03	1.19	2.37	0.04	4.36	100.38	346	33	27	12	7	8	11	86	6.7	71	7.2	55	20	131
HS6	CZ	51.44	0.41	11.44	16.54	0.27	2.53	1.16	0.65	2.79	0.05	11.83	99.12	367	38	41	11	10	12	14	98	27.0	60	12.4	145	40	131
HS7	FS	77.14	0.29	10.99	2.75	0.04	0.73	0.54	1.63	2.37	0.05	3.24	99.77	428	34	24	10	7	13	16	87	5.2	106	9.1	46	18	112
HS8	FS	78.09	0.25	10.29	2.41	0.05	0.72	0.71	1.60	2.22	0.05	3.36	99.73	405	33	23	8	7	8	13	80	4.6	106	8.9	46	17	107
HS9	MST	72.14	0.57	16.14	1.84	0.01	0.69	0.08	1.51	3.76	0.04	3.68	100.47	367	63	40	19	12	9	26	142	7.9	105	12.1	83	25	180
HS10	MST	68.78	0.70	17.45	1.96	0.01	0.76	0.08	1.28	4.35	0.04	3.98	99.41	406	65	51	20	14	7	21	162	6.9	114	13.4	87	23	182
Gohchidani Member																											
GH1	VFS	76.16	0.31	11.36	1.87	0.03	1.01	1.42	1.73	2.12	0.07	4.05	100.13	847	35	28	12	6	13	17	80	5.8	191	7.3	43	15	160
GH2	CZ	74.49	0.43	13.38	2.22	0.02	0.72	0.44	1.93	2.75	0.06	3.14	99.59	428	47	35	12	7	13	15	103	7.4	146	10.9	66	19	171
GH3	VFS	75.31	0.36	12.07	3.20	0.04	0.83	0.46	1.97	2.33	0.06	3.36	99.98	399	39	32	12	6	13	16	88	6.9	150	8.8	62	17	143
GH4	CZ	74.23	0.50	13.56	1.97	0.02	0.71	0.54	2.03	2.83	0.06	3.20	99.64	483	51	45	13	8	15	19	110	7.0	176	10.6	74	19	196
GH5	MST	64.44	0.78	16.87	4.60	0.05	1.68	0.31	1.37	4.30	0.07	5.68	100.14	604	69	117	20	15	60	26	167	13.9	75	14.2	126	32	148
GH6	MST	60.95	0.64	14.38	7.79	0.08	2.47	0.85	1.35	3.54	0.09	7.98	100.12	548	52	76	15	12	44	21	138	11.2	89	12.4	117	28	137
GH7	FS	73.93	0.30	10.59	2.34	0.05	1.11	2.55	2.09	2.42	0.06	4.56	100.01	691	31	32	10	6	16	20	83	6.8	180	6.8	41	17	142
GH8	VFS	75.88	0.40	12.43	2.97	0.01	0.84	0.15	2.34	2.41	0.07	2.13	99.62	547	46	41	11	9	14	19	87	5.1	119	9.7	58	15	170
GH8A	CZ	69.75	0.57	14.62	5.39	0.01	1.42	0.12	1.89	2.68	0.05	3.44	99.97	492	51	52	15	10	21	19	103	7.6	93	11.3	98	25	166
GH9	VFS	76.79	0.35	11.03	2.92	0.02	0.75	0.89	2.29	2.32	0.11	2.24	99.70	604	42	36	11	8	23	13	79	5.6	140	6.9	46	18	216
GH10	CZ	69.64	0.55	13.03	4.04	0.07	1.51	1.37	2.18	2.63	0.08	5.10	100.19	460	52	67	14	10	25	15	98	7.6	214	7.9	80	22	172
GH11	CZ	68.91	0.57	12.92	4.19	0.07	1.51	1.40	2.14	2.61	0.08	4.98	99.39	464	51	67	13	11	26	12	98	8.4	214	9.0	82	23	172
GH12	CZ	71.18	0.60	14.13	4.54	0.03	0.95	0.39	2.04	2.89	0.14	2.92	99.82	534	52	53	14	10	17	20	116	9.3	113	12.0	99	28	181
GH13	CZ	71.09	0.67	14.90	3.53	0.02	0.90	0.27	2.09	3.26	0.09	2.95	99.78	533	55	57	16	11	16	23	129	9.5	103	11.1	111	25	179
Shirahama Formation																											
S-1 Member																											
S1-1	VFS	82.68	0.19	10.33	0.67	0.01	0.29	0.16	1.72	2.62	0.03	1.37	100.07	443	36	26	9	4	6	17	86	2.4	93	7.8	19	13	224
S1-2	VFS	82.61	0.18	10.25	0.51	0.01	0.26	0.20	1.81	2.64	0.02	1.30	99.79	397	39	23	10	5	4	17	85	1.7	90	6.0	17	14	233
S1-3	FS	78.11	0.20	10.02	2.16	0.03	0.82	1.30	1.69	2.49	0.03	3.12	99.99	402	36	27	10	5	10	17	81	5.4	123	7.3	27	18	272
S1-4	FS	81.57	0.21	10.67	1.05	0.01	0.31	0.13	1.80	2.67	0.03	1.48	99.93	405	46	24	10	4	8	17	87	2.7	91	6.8	21	19	300
S1-5	MST	72.76	0.51	14.56	2.38	0.02	0.70	0.20	2.17	3.17	0.05	3.42	99.93	471	56	50	14	13	17	25	121	6.2	125	12.6	64	21	235
S1-6	MST	71.33	0.49	13.77	3.37	0.03	0.95	0.50	2.15	3.38	0.05	3.85	99.87	528	54	46	14	11	15	21	125	6.4	115	10.3	70	24	206
S1-7	VFS	78.54	0.25	10.89	1.79	0.02	0.54	0.96	2.44	2.50	0.03	2.52	100.48	439	44	30	10	5	10	19	84	3.3	138	7.7	30	16	222
S1-8	MST	65.75	0.75	17.76	3.69	0.02	1.04	0.21	1.39	4.59	0.05	4.61	99.85	495	71	72	21	16	21	24	184	11.1	93	16.1	115	30	159
S1-9	VFS	79.87	0.24	10.54	1.54	0.02	0.57	0.43	2.34	2.34	0.03	2.17	100.09	432	44	33	8	7	10	17	82	2.9	106	9.5	29	16	262
S1-10	MST	65.06	0.57	14.66	5.77	0.04	1.55	0.71	1.80	3.61	0.05	5.98	99.81	488	53	51	16	12	18	19	135	9.4	120	11.7	85	25	167
S-2 Member																											
S2-1	CZ	70.85	0.52	14.18	3.59	0.03	0.98	0.37	1.56	3.54	0.05	4.17	99.84	455	57	49	14	11	15	20	129	7.6	114	12.2	79	25	213
S2-2	FS	74.28	0.27	10.74	2.01	0.03	1.08	2.14	1.76	2.84	0.04	4.13	99.33	454	41	28	10	5	11	19	95	5.7	209	7.8	35	19	217
S2-3	VFS	80.61	0.24	11.46	0.67	0.01	0.45	0.46	2.25	2.70	0.03	1.68	100.56	454	43	29	10	7	7	18	89	1.6	108	8.6	24	15	259
S2-4	VFS	81.26	0.22	10.91	0.72	0.01	0.34	0.15	2.23	2.64	0.03	1.32	99.84	417	40	24	10	4	4	16	87	1.5	98	7.5	23	16	231
S2-5	VFS	81.23	0.24	11.08	0.62	0.01	0.33	0.44	2.22	2.49	0.04	1.53	100.21	442	42	22	10	5	5	19	84	2.3	117	8.3	25	15	304
S2-6	VFS	79.70	0.30	11.58	0.76	0.01	0.34	0.22	2.42	2.78	0.03	1.46	99.60	495	40	24	10	8	7	15	95	2.9	113	7.5	33	16	206
S2-7	MST	77.77	0.42	12.93	0.75	0.00	0.37	0.14	2.24	3.14	0.04	1.76	99.56	541	57	34	12	8	4	17	111	3.5	107	10.5	46	19	285
S2-8	FS	80.82	0.27	10.44	0.95	0.01	0.33	0.52	2.44	2.49	0.03	1.54	99.83	500	43	20	9	6	7	14	85	3.4	122	7.6	29	17	271
S-3 Member																											
S3-1	VFS	80.56	0.36	11.54	0.53	0.01	0.36	0.10	1.79	3.32	0.05	1.32	99.91	590	52	20	11	8	2	24	117	3.1	110	8.9	36	15	337
S3-2	FS	79.56	0.21	9.79	2.21	0.02	0.60	0.79	1.44	2.66	0.02	2.65	99.95	620	29	18	9	6	6	16	83	2.8	186	5.3	23	11	178
S3-3	FS	79.62	0.19	10.00	1.38	0.02	0.59	0.97	1.43	2.87	0.02	2.57	99.64	691	25	13	8	4	6	18	88	3.0	191	7.4	22	10	127
S3-4	FS	80.75	0.22	9.18	1.18	0.02	0.55	1.15	1.39	2.59	0.02	2.54	99.58	577	36	22	8	3	4	14	82	2.5	183	5.0	20	13	161
S3-5	VFS	71.28	0.30	10.12	2.74	0.06	1.62	4.61	1.46	2.41	0.02	5.30	99.92	493	39	22	10	7	7	13	81	6.9	219	7.1	27	22	265
S3-6	MST	61.25	0.65	15.36	8.44	0.11	4.43	0.86	1.17	2.30	0.14	5.02	99.73	255	63	61	17	13	46	21	97	11.2	67	12.3	110	39	202
S3-7	MST	70.13	0.67	16.23	3.52	0.03	1.16	0.09	1.44	3.48	0.04	3.18	99.97	430	68	56	17	13	14	15	143	8.8	60	13.5	86	24	231
S3-8	MST	70.34	0.66	16.34	3.14	0.03	1.09	0.10	1.49	3.64	0.04	3.17	100.05	433	68	57	17	13	19	17	148	7.9	64	14.5	91	25	229
S3-9	M SILL	70.06	0.32	10.16	3.69	0.06	1.91	4.57	1.33	2.24	0.03	5.51	99.88	404	46	23	10	5	10	14	80	8.4	240	7.6	39	19	242
S3-10	ZST	67.45	0.72	16.84	4.40	0.03	1.38	0.18	1.27	3.86	0.05	3.69	99.86	434	75	61	18	14	21	24	158	10.8	61	14.7	105	29	209
S3-MD	M DIKE	69.15	0.62	14.59	4.81	0.04	1.64	1.25	1.19	3.13	0.11	3.92	100.46	431	59	64	16	12	26	23	126	8.7	125	10.8	86	26	190
S-4 Member																											
S4-1	CS	63.70	0.05	5.60	0.68	0.03	4.96	10.59	0.43	1.53	0.03	11.84	99.44	412	17	3	5	1	3	10	42	8.4	312	3.7	5	7	58
S4-2	MS	64.72	0.09	6.52	0.83	0.02	5.55	7.36	0.66	1.82	0.09	11.95	99.62	402	16	6	6	2	2	15	55	7.1	155	3.7	6	9	80
S4-3	MS	72.01	0.10	7.05	1.26	0.09	2.95	4.73	0.47	1.99	0.03	8.86	99.54	596	17	11	6	2	2	13	63	5.6	176	4.6	10	13	88
S4-4	ZST	66.33	0.89	17.38	1.09	0.00	0.20	0.08	1.76	10.51	0.01	1.76	100.01	1989	35	40	15	19	3	16	309	9.8	105	17.3	70	24	248
S4-5	MS	83.63	0.14	9.09	0.19	0.00	0.14	0.02	1.66	3.91	0.00	0.78	99.57	811	14	8	9	2	<1	19	120	1.0	79	4.9	14	8	125
S4-6	MS	83.62	0.17	9.12	0.48	0.00	0.08	0.02	1.69	4.07	0.00	1.08	100.34	720	27	9	9	3	<1	23	128	1.0	76	5.0	12	11	172
S4-7	ZST	64.86	0.83	16.76	1.36	0.01	0.09	0.15	1.99	11.06	0.01	2.13	99.26	1965	41	29	8	18	9	20	332	9.3	147	19.2	58	38	221
S4-8	FS	84.44	0.12	8.27	0.81	0.00	0.07	0.01	1.52	3.86	0.00	1.28	100.39	675	21	9	7	2	1	18	125	1.3	70	2.8	12	6	112
S4-9	ZST	72.19	0.78	14.95	0.28	0.00	0.14	0.05	3.34	6.39	0.01	1.65	99.80	1285	37	31	14	15	1	13	198	8.2	128	12.6	52	21	260
S-5 Member																											
S5-1	MST	69.47	0.72	17.53	1.77	0.01	0.68	0.00	0.25	5.83	0.01	3.53	99.79	625	58	57	23	17	4	10	252	9.9	57	15.2	96	26	305
S5-2	MS-FS	84.94	0.13	8.54	0.40	0.00	0.17	0.00	0.10	4.05	0.00	1.16	99.51	674	15	14	7	2	1	11	140	0.6	59	5.1	13	6	101
S5-3	MS	84.87	0.15	8.96	0.51	0.01	0.18	0.00	0.05	4.37	0.00	1.06	100.17	726	23	18	8	4	<1	12	150	0.5	63	3.4	12	9	141
S5-4	MS	84.41	0.16	9.28	0.33	0.01	0.20	0.00	0.32	4.12	0.00	1.27	100.09	670	23	12	8	4	1	11	146	1.7	60	4.8	14	8	136
S5-5	mst	66.40	0.85	18.76	2.66	0.02	0.75	0.00	0.04	6.31	0.02	4.21	100.01	646	76	64	27	16	8	15	278	12.4	61	15.5	107	23	287
S5-6	mst	66.23	0.88	18.38	2.39	0.02	0.84	0.00	0.06	6.02	0.02	4.18	99.01	551	88	67	24	15	9	10	282	13.5	43	15.5	124	25	244

Table 2 ICP-MS REE and trace element analyses of Tanabe Group sedimentary rocks and GSJ standards included in the same runs. Sample numbers andlithologies as in Table 1. All data are p.p.m., reported as analysed (ignited basis).

SA#	LITH	La	Ce	Pr	Nd	Sm	Eu	Gd	Tb	Dy	Ho	Er	Tm	Yb	Lu	Hf	Ta	Th	U	Zr	Nb	Be	Sn	Sb
IW1	MS	9.28	19.73	2.12	7.73	1.50	0.41	1.50	0.22	1.33	0.25	0.66	0.10	0.73	0.11	1.97	0.25	3.75	0.82	72	2.66	0.64	0.81	0.22
IW2	MS	22.32	36.04	4.46	15.54	2.55	0.69	2.29	0.28	1.71	0.31	0.81	0.12	0.81	0.12	1.74	0.26	4.87	0.92	59	2.20	0.75	0.50	0.52
IW4	CS	14.01	30.44	3.21	11.78	2.16	0.50	1.94	0.28	1.66	0.32	0.90	0.16	1.04	0.16	2.96	0.44	5.68	1.18	117	4.46	1.04	1.14	0.28
IW5	FS	16.65	36.31	3.77	14.33	2.54	0.58	2.26	0.32	1.93	0.41	1.20	0.19	1.38	0.21	3.42	0.47	7.01	1.49	149	5.78	1.63	1.45	0.21
IW7	CZ	20.56	46.11	4.60	16.67	2.92	0.61	2.55	0.36	2.33	0.48	1.39	0.24	1.58	0.25	3.45	0.63	8.92	1.88	124	7.53	1.77	1.86	0.34
MA1	MST	26.68	59.53	6.44	25.18	5.42	1.13	5.41	0.81	4.87	0.96	2.61	0.41	2.78	0.42	5.57	0.88	12.25	2.74	207	10.62	2.34	2.37	0.42
MA2	FS	19.09	42.07	4.47	16.89	3.31	0.74	3.27	0.49	2.94	0.57	1.58	0.25	1.71	0.26	3.40	0.57	8.62	1.85	122	6.69	1.64	1.79	0.50
MA5	CZ	23.52	51.95	5.47	20.42	3.95	0.79	3.72	0.54	3.47	0.70	1.99	0.33	2.24	0.36	5.14	0.76	10.30	2.35	190	9.18	1.99	2.04	0.44
MA6	VFS	17.96	41.06	4.18	15.89	3.11	0.73	2.94	0.46	2.83	0.56	1.57	0.25	1.71	0.26	3.44	0.54	7.69	1.64	121	6.62	1.47	1.69	0.17
MA11	CZ	22.03	46.93	4.78	17.03	2.98	0.60	2.51	0.36	2.47	0.53	1.61	0.26	1.86	0.28	4.51	0.67	8.71	1.91	161	7.89	1.44	1.91	0.58
MA12	VFS	19.76	42.91	4.54	16.52	2.98	0.57	2.37	0.34	2.30	0.50	1.49	0.25	1.75	0.27	4.01	0.60	8.51	1.69	154	7.28	1.29	1.86	0.25
HS1	FS	16.61	35.64	3.76	14.07	2.69	0.57	2.54	0.37	2.34	0.45	1.28	0.20	1.40	0.21	3.31	0.50	7.20	1.47	121	5.63	1.33	1.65	0.18
HS4	CZ	26.61	59.12	6.34	23.60	4.63	0.90	4.40	0.69	4.42	0.90	2.52	0.40	2.73	0.42	5.25	0.88	12.02	2.75	192	10.58	2.55	2.52	0.39
HS5	FS	18.01	38.23	4.12	15.39	2.99	0.63	2.77	0.43	2.74	0.56	1.54	0.25	1.71	0.27	3.94	0.66	8.10	1.86	141	6.62	1.61	1.84	0.22
HS7	FS	18.18	39.23	4.29	16.20	3.15	0.68	2.99	0.44	2.67	0.53	1.44	0.23	1.56	0.23	3.24	0.57	7.96	1.60	116	6.48	1.52	1.69	0.24
HS9	MST	29.21	60.39	6.59	24.12	4.09	0.75	3.21	0.47	3.29	0.72	2.19	0.36	2.53	0.39	5.15	0.91	12.60	2.66	177	11.19	1.93	2.65	0.53
GH2	CZ	22.12	48.36	4.93	18.02	3.40	0.71	3.00	0.44	2.78	0.57	1.71	0.28	1.97	0.30	5.13	0.66	9.02	2.00	194	8.24	1.69	1.97	0.22
GH4	CZ	24.79	52.70	5.83	21.26	3.92	0.79	3.52	0.50	2.98	0.61	1.67	0.27	1.90	0.29	5.21	0.71	10.10	2.25	205	9.06	1.63	1.98	0.40
GH6	MST	30.68	67.20	7.14	27.22	5.32	1.09	5.02	0.77	4.66	0.93	2.60	0.41	2.75	0.41	4.42	1.04	12.88	2.77	153	12.20	2.30	2.83	0.65
GH7	FS	16.96	35.00	3.93	14.45	2.88	0.97	2.82	0.42	2.45	0.48	1.32	0.21	1.44	0.22	3.90	0.50	6.77	1.57	144	6.19	1.08	1.50	0.38
GH8	VFS	19.64	39.50	4.37	15.78	2.70	0.67	2.20	0.31	2.04	0.43	1.26	0.22	1.53	0.25	4.65	0.61	8.02	1.84	175	7.60	1.15	1.62	0.37
GH8A	CZ	27.31	57.19	6.18	22.86	4.09	0.81	3.47	0.55	3.74	0.79	2.27	0.36	2.47	0.38	4.68	0.84	10.91	2.52	168	10.91	1.68	2.24	0.52
GH12	CZ	27.47	59.78	6.45	24.79	4.98	1.11	4.71	0.68	4.14	0.81	2.21	0.35	2.35	0.36	4.81	0.84	10.72	2.38	194	10.58	1.84	2.28	0.50
GH13	CZ	27.34	51.50	5.93	21.82	3.95	0.80	3.44	0.53	3.39	0.71	2.04	0.34	2.31	0.35	4.59	0.86	11.71	2.34	169	11.43	2.11	2.36	0.38
S1-1	VFS	15.33	31.22	3.39	12.37	2.26	0.55	2.08	0.30	1.99	0.42	1.25	0.21	1.49	0.25	6.29	0.38	6.53	1.77	271	4.68	1.12	4.57	0.33
S1-2	VFS	15.44	32.34	3.47	12.75	2.31	0.51	2.04	0.30	1.93	0.40	1.18	0.21	1.49	0.24	6.63	0.38	6.71	1.76	266	4.58	1.17	1.26	0.23
S1-5	MST	28.39	56.71	6.32	23.40	4.39	0.81	3.85	0.55	3.42	0.69	1.99	0.33	2.34	0.36	6.84	0.86	11.97	2.65	287	10.37	1.88	2.28	0.49
S1-6	MST	26.20	54.23	5.96	22.27	4.16	0.86	3.84	0.56	3.58	0.71	2.05	0.33	2.36	0.36	5.97	0.80	10.91	2.58	244	10.12	1.82	2.12	0.30
S1-8	MST	36.62	72.91	8.31	31.05	5.60	0.96	4.70	0.72	4.54	0.92	2.62	0.42	2.88	0.44	4.57	1.10	16.16	3.04	150	14.20	3.25	3.29	0.35
S1-9	VFS	17.64	37.28	4.06	15.07	2.79	0.63	2.48	0.38	2.39	0.50	1.43	0.24	1.72	0.27	6.63	0.49	7.38	1.93	237	5.67	1.11	1.30	0.41
S2-1	CZ	27.77	60.63	6.46	24.08	4.64	0.91	4.08	0.60	3.79	0.76	2.10	0.34	2.37	0.37	5.84	0.90	11.74	2.73	244	10.87	2.26	2.43	0.36
S2-2	FS	18.50	41.15	4.42	16.61	3.35	0.79	3.33	0.52	3.14	0.60	1.63	0.26	1.76	0.28	6.36	0.51	7.93	1.92	265	6.05	1.16	1.38	0.38
S2-4	VFS	16.84	35.84	3.79	13.90	2.42	0.48	2.22	0.34	2.15	0.45	1.33	0.22	1.56	0.25	5.25	0.47	7.77	1.81	207	5.59	1.14	1.18	0.35
S2-6	VFS	18.13	38.49	4.11	14.83	2.80	0.62	2.52	0.38	2.37	0.48	1.40	0.23	1.66	0.25	5.28	0.56	7.75	1.94	203	6.83	1.25	1.46	0.24
S2-7	MST	23.11	49.10	5.28	19.61	3.51	0.71	3.02	0.43	2.75	0.56	1.72	0.29	2.00	0.31	7.53	0.71	9.49	2.26	295	8.70	1.27	1.69	0.37
S3-2	FS	14.37	29.19	3.14	11.13	2.11	0.56	1.94	0.28	1.70	0.33	0.90	0.15	1.06	0.17	4.59	0.40	5.09	1.14	171	4.79	1.07	1.04	0.20
S3-4	FS	17.27	34.20	3.79	13.66	2.49	0.62	2.23	0.33	2.03	0.39	1.06	0.17	1.21	0.17	3.41	0.39	5.53	1.08	138	4.71	0.89	0.99	0.21
S3-5	VFS	20.74	42.13	4.65	17.13	3.35	1.00	3.49	0.51	3.25	0.65	1.83	0.30	2.04	0.33	7.45	0.56	8.09	1.92	315	6.81	1.15	1.39	0.39
S3-7	MST	34.96	74.12	7.79	29.16	4.87	0.86	4.13	0.55	3.48	0.71	2.13	0.35	2.52	0.40	6.61	1.07	14.13	2.91	249	13.92	1.87	2.76	0.45
S3-8	MST	35.00	74.53	7.97	29.80	5.48	0.96	4.84	0.66	4.12	0.82	2.36	0.39	2.72	0.41	6.31	1.05	13.93	2.84	242	13.39	2.25	2.65	0.33
S3-9	M SILL	19.57	40.93	4.40	16.68	3.30	0.97	3.17	0.49	2.93	0.58	1.64	0.26	1.82	0.28	5.92	0.56	7.76	2.09	230	6.79	1.37	1.30	0.66
S3-10	ZST	36.83	80.67	8.57	31.68	6.02	1.11	5.52	0.78	4.74	0.93	2.58	0.40	2.85	0.43	6.18	1.14	14.85	3.06	236	14.38	2.48	3.08	0.39
S3-MD	M DIKE	31.30	65.30	7.24	26.56	5.09	1.07	4.75	0.68	4.12	0.79	2.19	0.36	2.43	0.37	5.64	0.95	12.24	2.61	218	11.81	2.20	2.55	0.59
S4-3	MS	11.50	23.32	2.58	9.45	1.86	0.63	1.83	0.30	1.90	0.38	1.10	0.18	1.20	0.18	2.67	0.31	4.72	0.90	102	2.98	1.10	0.68	0.27
S4-4	MS	23.07	34.48	4.91	19.36	3.43	0.84	3.04	0.45	3.02	0.67	2.14	0.38	2.88	0.47	6.80	1.46	18.32	3.10	224	18.00	1.37	3.69	2.25
S4-6	MS	12.70	25.91	2.88	10.33	1.94	0.51	1.77	0.24	1.39	0.28	0.84	0.14	1.06	0.17	3.77	0.48	5.27	1.13	146	4.20	0.66	0.81	0.57
S4-7	ZST	28.19	43.57	5.96	23.57	4.31	1.02	4.25	0.69	4.97	1.10	3.25	0.55	3.74	0.57	5.39	1.39	16.82	3.07	170	17.09	1.32	4.69	2.13
S4-8	FS	8.02	15.99	1.78	6.32	1.13	0.35	1.03	0.13	0.81	0.16	0.49	0.09	0.68	0.11	2.67	0.37	3.57	0.77	99	3.02	0.56	0.80	0.67
S4-9	ZST	21.94	44.58	4.91	17.47	3.20	0.75	3.01	0.44	2.96	0.66	2.16	0.39	2.94	0.47	7.22	1.44	13.98	3.76	260	16.79	1.43	4.85	2.89
S5-1	MST	32.83	71.94	7.06	26.36	4.77	0.99	4.38	0.64	4.15	0.87	2.62	0.45	3.24	0.51	8.59	1.39	17.03	3.68	661	16.90	2.58	3.93	2.22
S5-2	MS-FS	9.32	19.08	2.00	7.30	1.35	0.36	1.20	0.16	1.04	0.20	0.63	0.11	0.77	0.12	3.08	0.36	4.03	0.96	118	3.45	0.70	1.01	0.85
S5-3	MS	10.15	18.70	2.04	7.31	1.28	0.35	1.18	0.17	1.12	0.23	0.69	0.11	0.85	0.14	5.20	0.38	3.57	1.00	207	3.80	0.78	1.44	1.20
S5-4	MS	9.78	20.05	2.24	8.24	1.51	0.39	1.39	0.20	1.25	0.25	0.69	0.12	0.88	0.14	3.60	0.42	4.34	1.04	139	4.02	0.75	1.22	0.69
S5-5	MST	37.64	85.99	9.18	33.75	6.10	1.11	5.26	0.71	4.20	0.83	2.47	0.42	3.14	0.51	8.02	1.47	18.27	3.87	291	17.36	2.85	5.80	4.48

GSJ STANDARD ROCKS

STD		La	Ce	Pr	Nd	Sm	Eu	Gd	Tb	Dy	Ho	Er	Tm	Yb	Lu	Hf	Ta	Th	U	Zr	Nb	Be	Sn	Sb
JB-1b	Basalt	39.75	68.41	7.16	26.28	4.93	1.49	5.03	0.70	4.15	0.78	2.06	0.31	1.99	0.30	3.32	1.59	9.35	1.57	123	24.74	1.27	1.55	0.20
JB-1b		41.51	72.36	7.44	27.71	5.09	1.55	5.20	0.73	4.32	0.80	2.10	0.32	2.10	0.30	3.40	1.63	9.73	1.65	143	26.53	1.22	1.76	0.10
JB-1b		41.32	73.77	7.46	27.22	5.21	1.53	5.14	0.71	4.27	0.81	2.09	0.31	2.06	0.31	3.41	1.65	9.81	1.67	133	25.64	1.28	1.71	0.15
JB-1b		41.43	71.59	7.44	27.44	5.10	1.54	5.00	0.71	4.15	0.81	2.12	0.32	2.04	0.31	3.37	1.68	9.62	1.62	127	25.53	1.26	1.71	0.14
JB-1b		39.08	68.55	7.09	25.75	4.78	1.47	4.81	0.68	4.12	0.77	2.05	0.30	1.98	0.28	3.27	1.57	9.27	1.61	128	25.81	1.32	1.69	0.10
JB-1b		39.80	68.25	7.15	26.21	4.95	1.49	5.08	0.69	4.12	0.78	2.05	0.31	1.97	0.30	3.29	1.70	9.39	1.61	133	25.99	1.29	1.79	0.13
Average		40.48	70.49	7.29	26.77	5.01	1.51	5.04	0.70	4.19	0.79	2.08	0.31	2.02	0.30	3.35	1.63	9.53	1.62	131	25.71	1.27	1.70	0.14
StdDev		2.12	4.78	0.35	1.58	0.31	0.06	0.27	0.03	0.17	0.04	0.06	0.01	0.10	0.02	0.12	0.10	0.45	0.07	14	1.18	0.07	0.16	0.08
CV%		5.24	6.78	4.76	5.91	6.18	4.01	5.30	4.48	3.97	4.56	2.78	4.37	5.13	7.04	3.60	6.14	4.68	4.06	10	4.59	5.37	9.67	55.29
RV(JB-1a)		*37.60*	*65.90*	*7.30*	*26.00*	*5.07*	*1.46*	*4.67*	*0.69*	*3.99*	*0.71*	*2.18*	*0.33*	*2.10*	*0.33*	*3.41*	*1.93*	*9.03*	*1.57*	*144*	*26.90*	*1.44*	*2.24*	*0.25*
JB-1	Basalt	38.49	68.07	7.08	26.28	4.97	1.52	5.14	0.71	4.33	0.81	2.13	0.33	2.14	0.31	3.56	2.51	9.40	1.67	136	33.98	1.38	2.07	0.27
RV		*38.60*	*67.80*	*7.01*	*26.80*	*5.13*	*1.49*	*4.90*	*0.82*	*4.14*	*0.79*	*2.27*	*0.35*	*2.13*	*0.31*	*3.31*	*2.93*	*9.30*	*1.67*	*141*	*33.30*	*1.33*	*1.92*	*0.28*
JG-2	Granite	19.41	40.14	6.01	24.91	7.67	0.08	8.51	1.53	10.42	2.25	6.13	1.01	6.90	1.02	3.74	2.02	29.19	9.32	78	13.98	3.25	2.04	0.04
RV		*19.90*	*48.30*	*6.20*	*26.40*	*7.78*	*0.10*	*8.01*	*1.62*	*10.50*	*1.67*	*6.04*	*1.16*	*6.85*	*1.22*	*4.73*	*2.76*	*31.60*	*11.30*	*98*	*14.70*	*3.26*	*3.00*	*0.06*
JG-1a	Granite	24.67	52.06	5.75	21.51	4.70	0.72	4.68	0.74	4.76	0.96	2.63	0.43	2.88	0.43	3.92	1.71	14.00	4.75	131	10.85	3.29	3.74	0.06
RV		*21.30*	*45.00*	*5.63*	*20.40*	*4.53*	*0.70*	*4.08*	*0.81*	*4.44*	*0.82*	*2.57*	*0.38*	*2.70*	*0.44*	*3.59*	*1.90*	*12.80*	*4.69*	*118*	*11.40*	*3.16*	*4.47*	*0.05*

Notes: [1] JB-1b results are six separate digests prepared at the same time as the Tanabe samples.
StdDev=Standard deviation (2 sigma); CV%=coefficient of variation.
No RVs are available for JB-1b, so the comparison is with its predecessor, JB-1a.
[2] JB-1b, JG-2 and JG-1a analysed on an ignited basis, JB-1 hydrous basis.
[3] Recommended values (RV) for GSJ standards from Imai et al. (1995).

1. Comparison between XRF and ICP-MS results

Seven elements (Zr, Nb, Th, Ba, Pb, Y and Ce) were determined by both methods. Agreement is excellent for both Zr and Nb (Fig. 3). This is significant, because the possibility of incomplete recovery of HFSE is always present when using dissolution techniques. The comparability of the Zr and Nb data, and the good agreement between the ICP-MS results for GSJ standards run concurrently and their recommended values (Table 2) suggest that recovery of the HSFE is complete using the digestion methods employed here. Thorium results are also well correlated, but XRF values are uniformly greater (+1.3 ppm) than those

from ICP-MS. This probably reflects a calibration and background bias in the XRF results. The XRF data are also inherently less precise, and the ICP-MS data are thus preferred. To ensure that the Th data in samples not analysed by ICP-MS are comparable, all Th data in Table 1 have been corrected by cross-calibration against the ICP-MS data (Fig. 3).

Ba and Pb analyses by routine solution ICP-MS can be problematic, because of high concentrations even at the dilutions analysed (Ba) or from volatility during acid digestion and alkali fusion (Pb). These features are clearly shown by comparison of the Ba and Pb results (Fig. 4). ICP-MS Ba results above 600 ppm are not plotted, because they are known to be high due to counter saturation. It is evident, however, that this effect also influences results between 500 and 600 ppm, with the ICP-MS results beginning to diverge to higher values. Consequently, the ICP-MS Ba analyses can only be considered accurate below 500 ppm. In contrast, virtually all ICP-MS Pb results are lower than those by XRF (Fig. 4). This strongly suggests loss of Pb during alkali fusion and acid digestion. Because of the above features, the XRF results are preferred, and the ICP-MS Ba and Pb data are not included in Table 2.

Ce and Y results show some differences between the techniques. The relationship for Ce is linear, but the nominal XRF results ex-machine were only comparable with those from ICP-MS between 35 and 65 ppm. Most of the Tanabe samples fall within this range. However, divergence outside of that was significant. ICP-MS results for the GSJ standards compare well with the recommended values (Table 2). This and the complete recovery of HFSE in the ICP-MS AFAD digestion suggest that the problem lay with the XRF data, possibly due to low count rates. Consequently, all Ce data in Table 1 have been cross-calibrated against the Tanabe ICP-MS data to ensure comparability within the dataset. Similar correction to the subset of Shimanto samples analysed at the same time also made that data comparable with the values determined earlier by Roser et al. (1998a).

The ICP-MS yttrium data were consistently low (-20% relative) in the Tanabe samples compared to the XRF results. This was also the case for the GSJ standards (average deviation from recommended values of -16.4%). This is apparently due to methodological bias. Munker (1997; in Robinson et al. 1999) found ICP-MS results to be 10-15% lower than XRF data for the same samples; other workers have also reported low ICP-MS results. Robinson et al. (1999) found a 9% discrepancy between ICP-MS results for USGS standards rocks and published values. However, their XRF data derived from calibrations based on synthetic Y standards agreed with the ICP-MS data. They interpreted this as reflecting bias towards high values in the recommended results for the USGS standard rocks, which are derived mainly from XRF data acquired from calibrations using natural rock reference materials. This accounts for the methodological discrepancy observed here, and suggests that the recommended values for the GSJ standards are also likely to be systematically high. We have carried out tests using XRF calibrations based on synthetic Y standards, and also find a discrepancy with our XRF calibration built solely on GSJ and USGS standard rocks. This finding agrees with that of Robinson et al. (1999). Our XRF results are thus likely to be systematically high. Because our tests are incomplete and we have not as yet derived precise correction factors, as an interim measure we have adopted the XRF values (Table 1) as analysed, to maintain internal consistency and comparability with the Shimanto data of Roser et al. (1998a) and other published XRF results. The comparability issue will be addressed further in a future paper.

REE results for the GSJ standards compare very well with the preferred values of Imai et al. (1995) (Table 2 and Fig. 5). This verifies that recovery of the HFSE in the alkali fusion and acid digestion was complete.

2. Tanabe Group: General elemental abundances

Traditional variation diagrams using Al_2O_3 as the abscissa are a useful screening technique to determine the extent of sorting fraction in sedimentary suites, and allow simple comparisons between groups. Example variation diagrams are given in Fig. 6 (major elements) and Figs. 7 and 8 (trace elements), plotted by formation and lithotype (sandstones and mudrocks). These plots also permit comparison with elemental abundances in the Shimanto sediments which are thought to comprise a major part of the Tanabe source.

(1) Major elements

The plots show marked sorting fractionation between sand and mud, with a clear division between sandstones and mudrocks, and almost no overlap at around 13.5 wt% Al_2O_3 (Fig. 6). SiO_2 contents range from about 65% in the most aluminous mudrocks to over 85 wt% in the sandstones. This range is comparable with that seen in the Shimanto terrane Otonashigawa and Muro Groups (Fig. 6), which form the majority of the clasts in Tanabe conglomerates. Most Tanabe samples lie along a linear detrital trend (DT), which is typical of relatively mature quartzose sediments, and are slightly more siliceous at given Al_2O_3 than their Shimanto protoliths, suggesting increase in detrital quartz during recycling. A few samples, however, scatter to lower values away from DT along dilution lines (DIL), suggesting presence of additional phases which do not contain Si and Al.

TiO_2 forms a tight linear trend, which intersects the

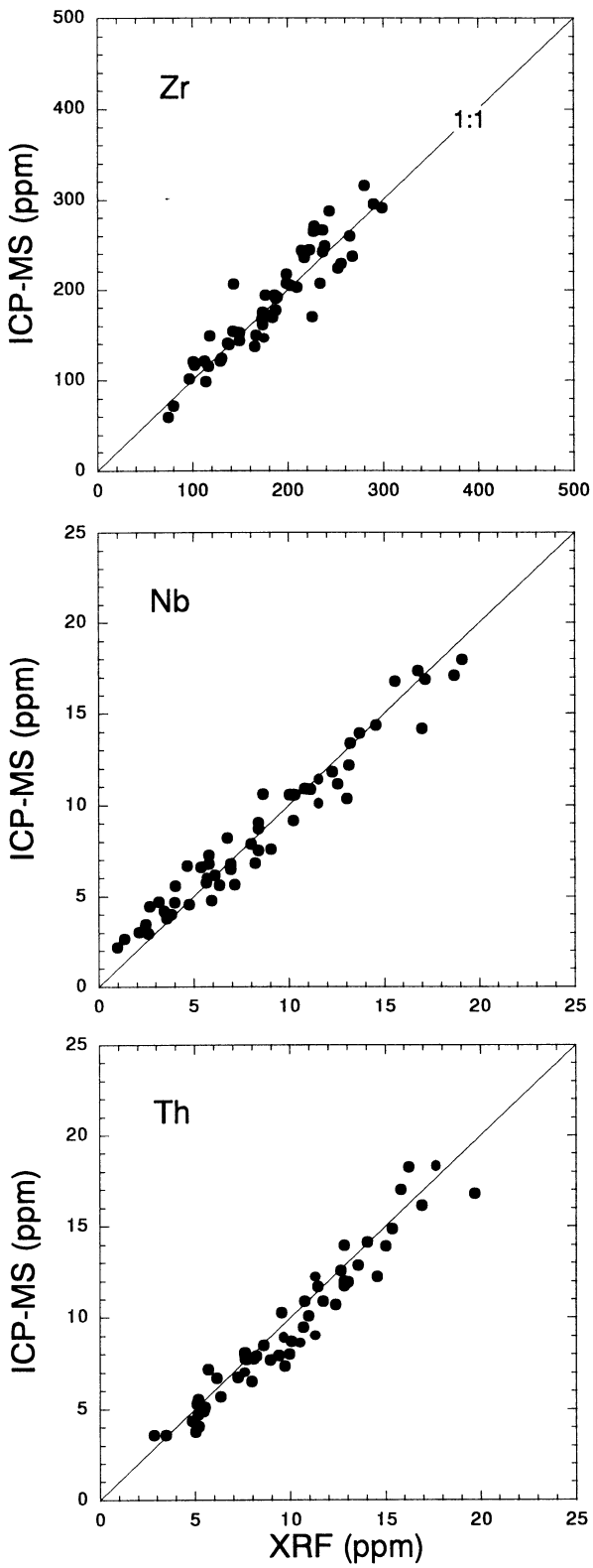

Fig. 3. Comparison of Zr, Nb and Th results for Tanabe Group samples analysed by both XRF and solution ICP–MS. XRF results on the Th plot have been corrected by −1.35 ppm, as outlined in the text.

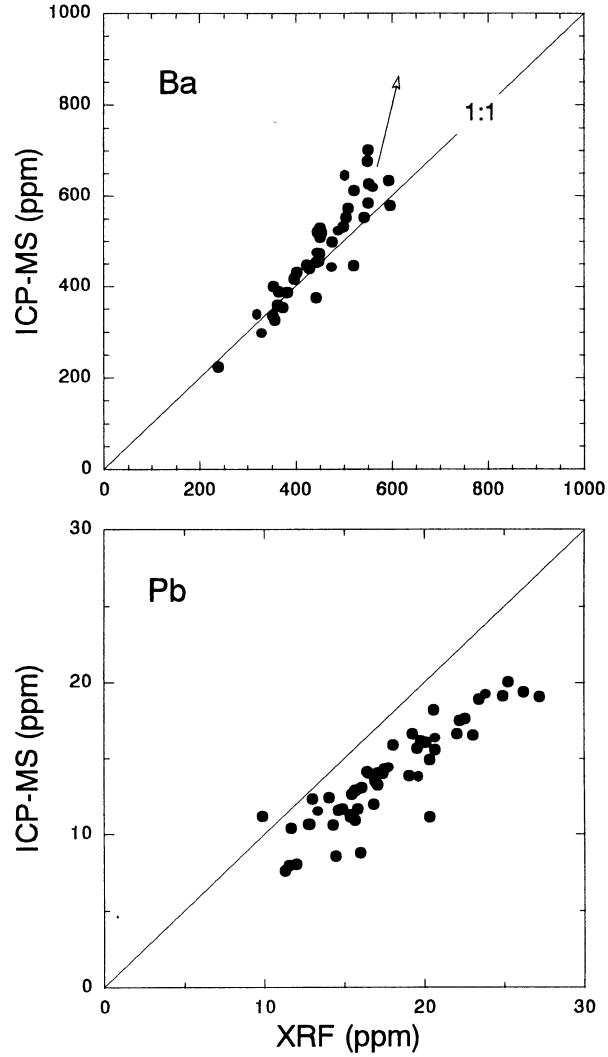

Fig. 4. Comparison of Ba and Pb results for Tanabe Group samples analysed by both XRF and solution ICP–MS. Samples with Ba >600 ppm are not plotted.

abscissa at around 7% Al_2O_3 (Fig. 6). This trend differs markedly from that expected from simple silica dilution (SDL), which is sometimes seen in highly mature quartz–clay systems or siliceous hemipelagic sediments. The strong correlation between Ti and Al attests to their immobility in geologic systems, and results from sorting fractionation of aluminous clays from sand-sized detritus. Intersection with the abscissa shows that significant amounts of aluminous framework grains (feldspar and rock fragments) remain in the Tanabe sediments. Published modal data for Tanabe sandstones are few, but many modal analyses have been made of coeval and comparable sediments in the nearby Kumano Basin. Kumano Group sandstones average $Q_{68}F_{24}R_8$ (Chijiwa 1992). The major element chemistry of the Tanabe samples is consistent with such values. The Tanabe samples show a similar trend to the Shimanto protolith, but are slightly depleted in TiO_2 at given Al_2O_3.

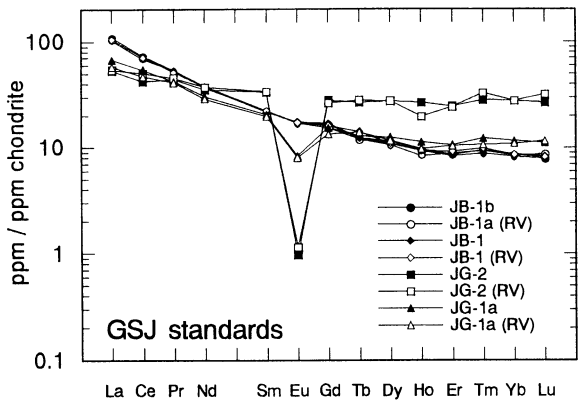

Fig. 5. Comparison of ICP-MS REE results for GSJ rock standards (Table 2) compared to GSJ preferred values. Chondritic normalising values from Taylor and McLennan (1985).

K_2O (Fig. 6) and MgO also show relatively strong correlation with Al_2O_3, reflecting primary residence in the clay fraction. For both, however, a small number of samples from the Shirahama Formation scatter to higher values, suggestive of diagenetic or other postdepositional redistribution. The K_2O plot is also clearly kinked at the sand/mudrock boundary, similar to the Shimanto protolith. This reflects differing mineralogical control in the sands (K-feldspar) compared to the muds (illitic clays). The Tanabe samples in general are slightly more potassic than the Shimanto suites, tending to plot at the upper end of the distribution. This suggests slightly more intense illitisation. Fe_2O_3T contents (not illustrated) show weak positive correlation and considerable scatter, but are broadly comparable with the Shimanto protoliths. In detail, Asso Fe data are quite well correlated, lying along what we interpret as the detrital trend. Shirahama data contribute most to the scatter, with contents in the mudrocks being markedly lower than Asso equivalents. This suggests significant provenance change in the Shirahama Formation or postdepositional depletion of Fe.

In contrast, Na_2O (Fig. 6) and CaO and show weak negative correlation with Al_2O_3. This pattern is typical of residence of these elements in plagioclase feldspar, and greater abundances of this mineral in sands than in muds. The Tanabe samples are generally depleted in Na_2O compared to the Shimanto suites, suggesting loss of albite during source weathering or recycling. A number of samples scatter to higher CaO, reflecting sporadic carbonate enrichment. This accounts for most of the samples which fall on dilution trends on the SiO_2 plot. MnO and P_2O_5 (not illustrated) display very weak positive correlations, and

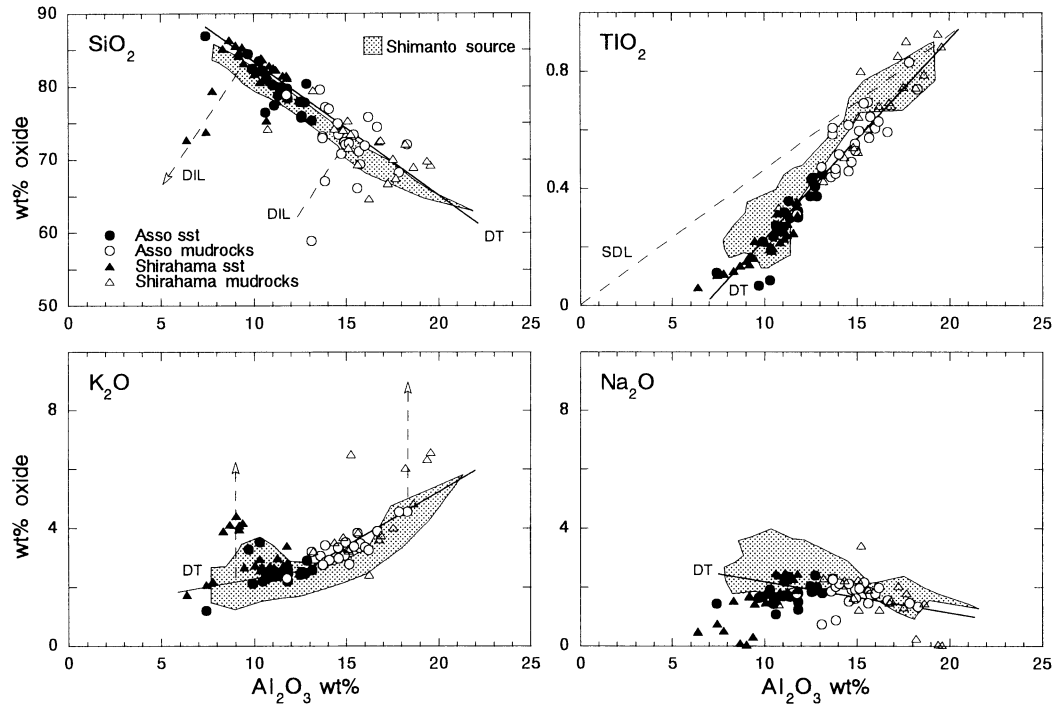

Fig. 6. Example major element-Al_2O_3 variation diagrams (anhydrous normalised basis) for Asso and Shirahama sandstones and mudrocks, compared to probable Shimanto source rocks. Solid line DT= detrital trend (fitted by eye); dashed line SDL= ideal silica dilution trend. Dashed arrows indicate directions of depletion (DIL) or enrichment from the detrital trend. Shaded field: distribution of sandstones and mudrocks from the Nyunokawa, Otonashigawa, and Muro suites of the Shimanto terrane (data of Roser et al. 1998a). Nyunokawa Formation (Hidakagawa Group) samples are included because they are similar chemically to the Otonashigawa Group, and distinct from the more volcanogenic inboard Hidakagawa formations (Yukawa, Terasoma, Miyama and Ryujin).

scatter to depleted values in the mudrocks similar to that shown for Fe. As with Fe, this depletion is a little more marked in the Shirahama Formation.

(2) Trace elements

The trace elements analysed by XRF can be divided into three groups on the basis of their trends on variation diagrams. The first and largest group (Ce, Cr, Ga, Nb, Rb, Sc, Ni, Th, Y, and V) shows strong positive correlations with Al, reflecting primary residence in the clay fraction. All of this group except Rb and perhaps Ni, Cr and V are resistant to redistribution by weathering or diagenesis, and hence display the strongest linear correlations. Abundances are also comparable with those in the Shimanto protolith, as shown by plots of Rb, Nb, Th and Y (Fig. 7). The Rb trend is kinked at the sand – mudrock boundary, reflecting contrasting mineralogical control and sorting (K-feldspar in sandstones; illitic clays in mudrocks), and enhanced diagenetic K-metasomatism in the finer sediments. Ga and Nb also exhibit similar but less pronounced kinks. Their immobile nature suggests the cause is related to detrital mineralogy. Ni data in the Shirahama Formation show some depletion in the mudrocks, similar to the pattern shown by Fe and Mn.

The second group (Ba, Pb, Sr) shows considerable scatter, and a tendency for abundances in the sandstones to be equal to or greater those in the mudrocks (Fig. 8). This suggests negative correlation with Al_2O_3, and hence association with feldspathic sand-sized detritus. All three elements can also be redistributed during diagenesis, which may have contributed to the scatter. Nevertheless, abundances are broadly similar with the Shimanto protolith suites (Fig. 8).

The third group is represented only by Zr. Asso Formation samples show a linear correlation with Al_2O_3, with abundances in mudrocks double those in sandstones (Fig. 8). This pattern is unusual, as Zr abundances in mineralogically mature suites such as these are usually controlled by detrital zircon. This typically produces scattered distributions, with weak maximums in the very fine or fine sands in which zircons are preferentially concentrated. There is no evidence of this in the Asso Formation, implying either residence in the clay fraction, or advanced zircon comminution to very fine size grades coupled with uniform distribution in both sands and mudrocks. Shirahama samples, however, show a more normal pattern, with scatter to high values in sandstones between 10–13 wt% Al_2O_3, reflecting zircon concentration. Abundances in Shirahama sandstones are two to three times higher than in Asso equivalents. Mudrocks are also uniformly enriched, but to a lesser extent. Abundances in Shirahama sandstones also closely correspond to those in Shimanto Muro Group sandstones, whereas those in the Asso sands match levels in Otonashigawa and Nyunokawa sandstones (Fig. 8).

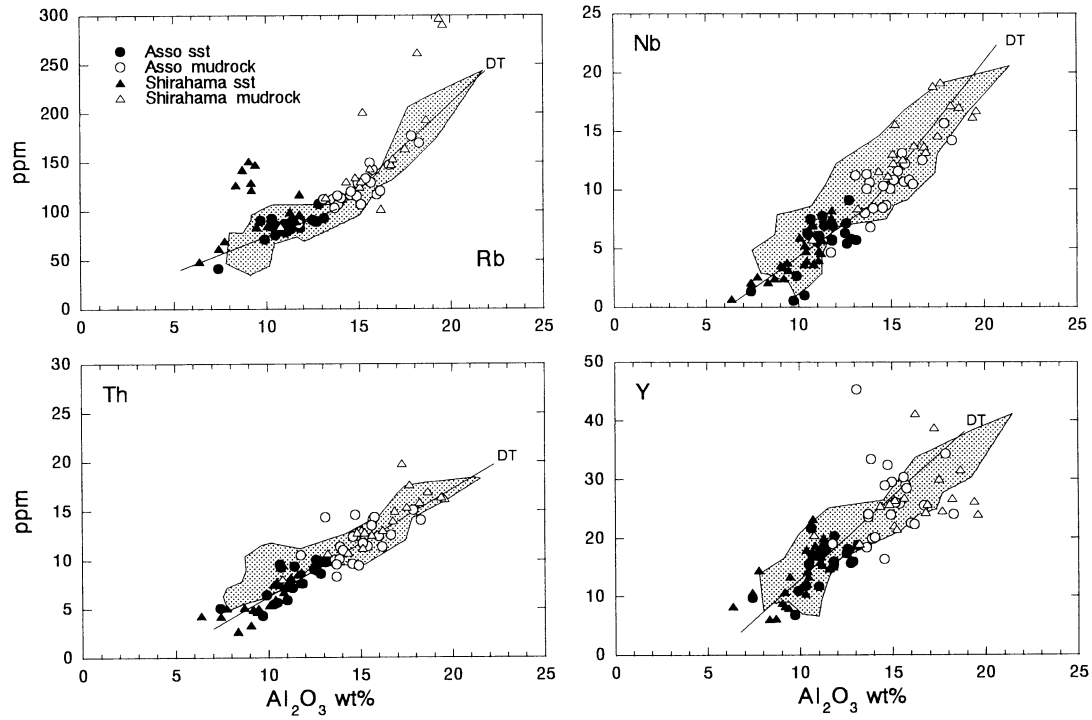

Fig. 7. Examples of trace elements, positively correlated with Al_2O_3 (anhydrous normalised basis). DT and distribution of Shimanto protoliths (shaded field) as in Fig. 7.

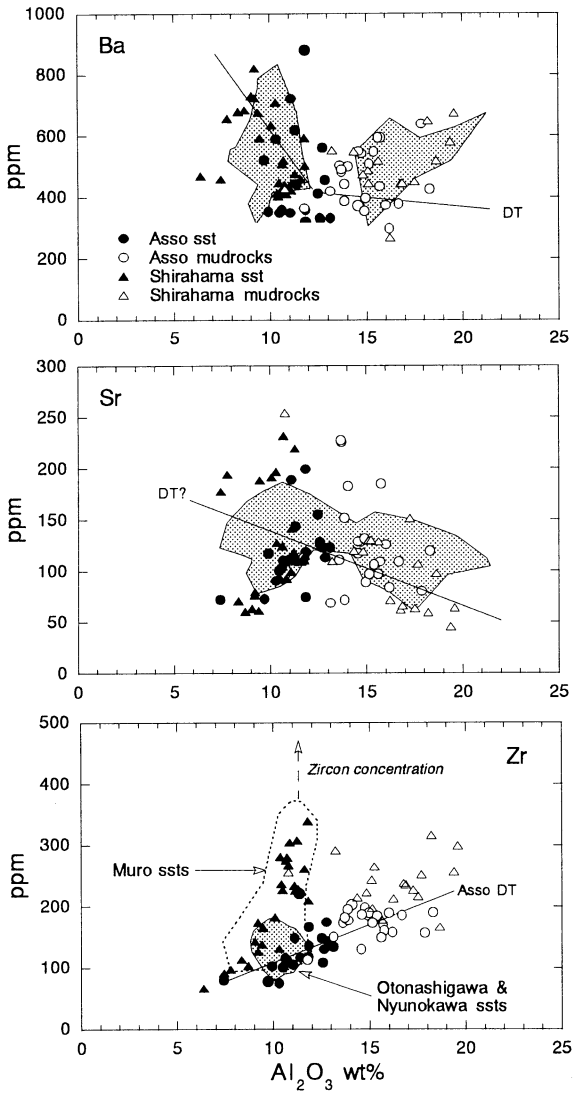

Fig. 8. Covariation of Ba, Sr and Zr with Al_2O_3 (anhydrous normalised basis). Shimanto protoliths (shaded field) on the Ba and Sr plots as in Fig. 7; individual fields for Otonashigawa–Nyunokawa sandstones (shaded) and Muro Group sandstones (dashed field) are differentiated on the Zr plot.

(3) REE

Chondrite-normalised plots of average REE abundances in average sandstones and mudrocks in each member of the Asso and Shirahama Formations are given in Fig. 9. Average Upper Continental Crust (UCC) and averages for Shimanto sediments are also plotted for comparison. Mudrocks in both the Asso and Shirahama Formations show similar patterns, with relatively high LREE enrichment and moderate europium anomalies. The patterns compare well with UCC and the Shimanto mudrock averages, reflecting derivation from a felsic continental margin source. Significant HREE enrichment (Tm–Lu) is evident in the upper members of the Shirahama Formation however, with patterns climbing above UCC and the Shimanto sandstone averages. This pattern is consistent with concentration of zircons and garnets, which are characteristically enriched in HREE (Taylor and McLennan 1985).

REE in the sandstones are strongly depleted relative to UCC, with La_N abundances falling to as low as 30 times chondrite, and HREE to as little as 2–3 times. Abundances are similar to or less than those in the average young Shimanto suites plotted. Older Shimanto sandstones (Campanian–Maastricthian and older; Yukawa to Ryujin Formations) have higher REE patterns very similar to UCC. The far lower abundances in the Tanabe averages are suggestive of dilution effect from increase in detrital quartz. This is also reflected by the relative fractionation between sandstone and mudstone, which is more marked in the Shirahama averages than in the Asso data. Almost all the sandstone averages exhibit HREE enrichment, which is particularly pronounced in the Shirahama S 4 and S 5 members. Preliminary REE modeling suggests that the HREE enrichments could be produced by very modest (0.05 and 0.07 volume per cent) concentrations of influxes of zircon and garnet, respectively (Roser et al. 2000). Progressive reduction in Eu anomaly stratigraphically upward is a notable feature of the Shirahama data. At present, the cause for this is unknown. Influx of mafic detritus or concentration of plagioclase and/or epidote could produce this effect, but there is no petrographic evidence to support these options.

Elemental Abundances: Significance

General elemental abundances and trends show marked sorting fractionation, as expected from the mineralogical and sedimentological maturity of the Tanabe sediments. The trends produced are consistent with separation of quartz–feldspar–lithic sand-sized detritus from aluminous silt and mud. The trends, extent of fractionation, and the elemental groupings shown by the variation diagrams are comparable with the Shimanto Otonashigawa and Muro Group sediments which were large components of the Tanabe source. In detail, however, some contrasts are evident. Fractionation is more advanced in the Shirahama Formation than in the Asso Formation, as shown by greater spread in abundances. For most elements, nearly all Shirahama mudrocks have higher abundances than Asso equivalents. Shirahama sandstones also spread to lower abundances than the Asso sands. This increased fractionation between sand and mud is also clearly shown by the REE, and is likely to be a product of winnowing in the storm-dominated shelf environment of the upper part of the Tanabe Group. Contrasting behaviour of Zr also show that significant differences occur in chemistry between the transgressive and regressive parts of the Tanabe sequence. These features suggest that significant modification of the bulk chemistry of clastic sediments can occur in shallow water forearc

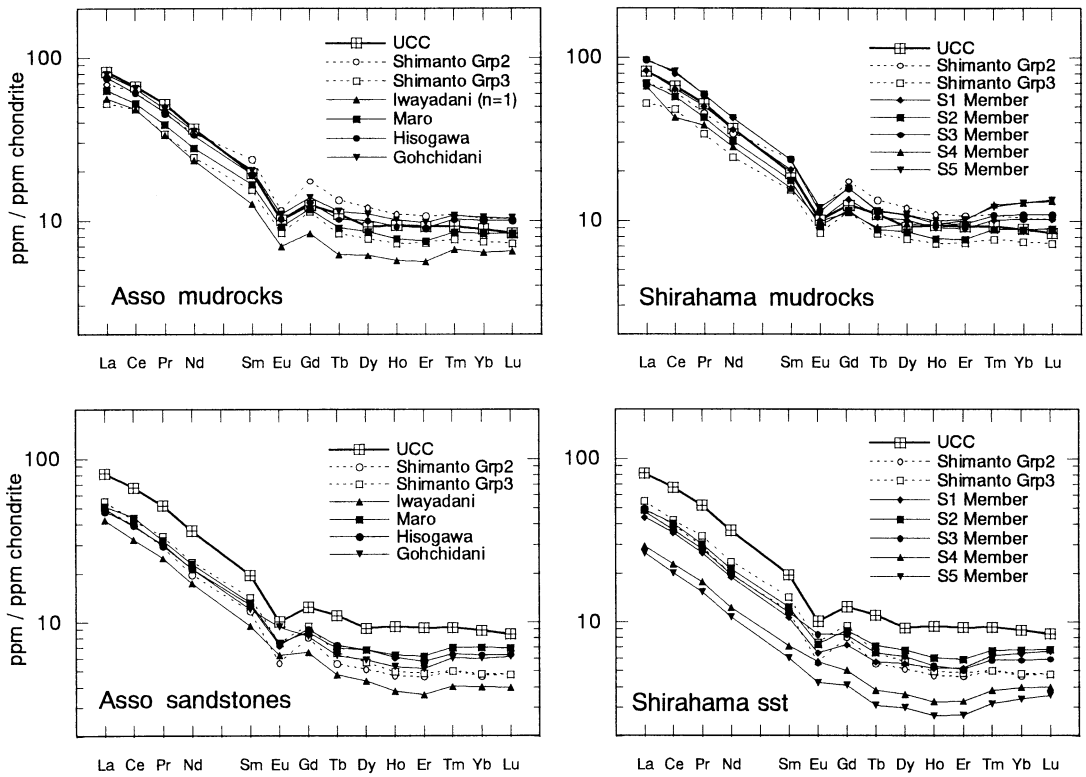

Fig. 9. Chondrite-normalised plots of average REE abundances in sandstones and mudrocks from the Tanabe Group, compared to UCC and Shimanto averages. Maro and Hisogawa averages include data for time-equivalent Gohchidani samples. Chondritic values and UCC (average Upper Continental Crust) from Taylor and McLennan (1985). Shimanto averages from Roser & Kimura (unpublished data): Grp 2=Nyunokawa Formation and Otonashigawa Group; Grp 3= Muro Group.

settings. The nature of these modifications and their implications will be discussed in more detail in a future paper.

Acknowledgements

Our thanks to Yoshihiro Sawada of Shimane University for access to the XRF equipment. This work was supported by funding from the Technical Research Center of the Japan National Oil Corporation.

References

Chijiwa, K. 1992. Detrital composition and sedimentary facies of the Miocene Kumano Group in the Outer Zone, Southwest Japan. *Memoirs of the Geological Society of Japan*, **38**, 311-327.*

Hisatomi, K. 1998. The importance of the sedimentary facies analysis in the research of stratigraphy - Instructions in the history of the Tanabe Group. *Earth Science (Chikyu Kagaku)*, **52**, 356-369.*

Imai, N., Terashima, S., Itoh, S. and Ando, A. 1995. 1994 compilation values for GSJ reference samples, "Igneous rock series". *Geochemical Journal*, **29**, 91-95.

Kimura, J.-I. and Yamada, Y. 1996. Evaluation of major and trace element analyses using a flux to sample ratio of two to one glass beads. *Journal of Mineralogy, Petrology and Economic Geology*, **91**, 62-72.

Munker, C. 1997. Geochemical and isotopic systematics of the Cambrian Devil River Volcanics in the Takaka Terrane, New Zealand. Ph.D. thesis, University of Göttingen, Germany.

Robinson, P., Townsend, A. T., Yu, Z. and Münker, C. 1999. Determination of scandium, yttrium and rare earth elements by high resolution inductively coupled plasma-mass spectrometry. *Geostandards Newsletter*, 23, 31-46.

Roser, B. P., Kimura, J.-I. and Hisatomi, K. 2000. Geochemical provenance signatures in Tanabe Group sediments, Wakayama. Geological Society of Japan, 107th Annual Meeting (Matsue), Abstracts, p. 79.

Roser, B. P., Ishiga, H., Bessho, T. and Dozen, K. 1998a. Major and trace element analyses of Cretaceous to Miocene sedimentary rocks from the Shimanto terrane, Kii Peninsula, SW Japan. *Geoscience Reports of Shimane University*, **17**, 13-24.

Roser, B. P., Sawada, Y. and Kabeto, K. 1998b. Crushing performance and contamination trials of a tungsten carbide ring mill compared to agate grinding. *Geoscience Reports of Shimane University*, **17**, 1-11.

Shimizu, H. and Hisatomi, K. 1993. Deformational mechanism of storm-origin sandstone. *Gekkan Chikyu*, **8**, 189-196.**

Shimizu, H. 1985. Pebbly mudstone diapirs of the Tanabe Group in the Kii Peninsula, southwest Japan. *Journal of the Geological Society of Japan*, **91**, 691-697.

Tanabe Research Group 1984. Stratigraphy and geological structure of the Tanabe Group in the Kii Peninsula, southwest Japan. *Earth Science (Chikyu Kagaku)*, **38**, 249-263.*

Tanabe Research Group 1985. Tanabe Group in the western coastal region (Hiki-Kamoi area) of the Kii Peninsula. *Memoirs of the Faculty of Education, Wakayama University, Natural Science*, **34**, 3-24.*

Tanabe Research Group 1992. Sedimentary facies and stratigraphy of the Asso Formation - Study on the Asso Formation, Tanabe Group (Part 1). *Earth Science (Chikyu Kagaku)*, **46**, 369-383.*

Tanabe Research Group 1993. Sedimentary facies and sedimentary

environments of the Shimomisu fan – delta – Study on the Asso Formation, Tanabe Group (Part 1). *Earth Science (Chikyu Kagaku)*, **47**, 1-16.*

Taylor, S. R. and McLennan, S. M. 1985. The continental crust: its composition and evolution. Oxford, Blackwell Scientific, 312 pp.

* in Japanese, English abstract.
** in Japanese.

(Received: 13 Oct.2000, Accepted: 20 Nov.2000)

（要　旨）

Barry Roser・木村純一・久富邦彦，2001，紀伊半島田辺層群の砂岩と泥質岩の全岩元素組成，島根大学地球資源環境学研究報告，19，101–112

珪質砕屑岩類である下部中新統の田辺層群は，和歌山県紀伊半島の南西部に露出する．この田辺層群は，上昇した四万十付加帯コンプレックスの上位に堆積した前弧盆のサクセッションである．本論では，田辺層群の層序に沿って採取した砂岩および泥質岩87試料の全岩蛍光X線分析結果を報告する．さらに，54試料を酸分解－アルカリ融解ICPMS法によって分析した．田辺層群の基部をなす朝来累層の分析結果は砂岩と泥質岩の間で特徴ある元素分析を示し，その傾向は上位の白浜累層でより顕著になる．これはおそらく暴浪の卓越した沿海環境での洗い出しによるとみられる．また，元素濃度は全般的に田辺層群の供給源となっている四万十帯のプロトリスと良く似ている．